Experimental Evaluation of Matrix Converter for Wind Energy Conversion System under Various Abnormal Conditions

Vinod Kumar*‡, R. R. Joshi*, R. C. Bansal**

*Department of Electrical Engineering, College of Technology and Engineering, India

**Department of Electrical, Electronics and Computer Engineering, University of Pretoria, South Africa

(vinodcte@yahoo.co.in, rrjoshi_iitd@yahoo.com, ramesh_bansal@up.ac.za)

‡ Corresponding Author; Vinod Kumar, MPUAT, Udaipur, 313001 India, vinodcte@yahoo.co.in

Received: 22.11.2013 Accepted: 05.01.2014

Abstract- This paper presents the experimental evaluation of reversed indirect matrix converter (MC) interfaced wind energy conversion system (WECS), where space vector pulse width modulation together with adaptive fuzzy logic control is effectively used to enhance the performance of system under various abnormal conditions like abrupt change in wind speed, disconnection from grid, misfire in the converter, sudden out of one phase, change in load etc. The proposed adaptive control system is realized using dSPACE DS1104 board. Selective experimental results are presented using a laboratory 1.2 kW prototype of WECS to demonstrate the resulting improvements of the developed system under abnormal conditions.

Keywords- Wind emulator, wind energy conversion system (WECS), Matrix converter, space vector pulse width modulation (SVPWM)

1. Introduction

In applications like advanced motor drives, power quality devices, electronic transformers, and distributed generation (DG) has high requirement for ac to ac power conversion. In DG, small decentralized sources like WECS, diesel generators, and micro-turbines are tied to the utility grid. Direct connection of such power sources to the utility grid is usually not possible because of magnitude and frequency constraints, and thus efficient ac to ac power converters are required for interfacing such power sources with utility grid.

For this purpose, ac-dc-ac converter [1-5] and matrix converter [6-11] are the two investigated matured choices. Although ac-dc-ac converter has high energy density and is relatively low in price, however has serious concerned with its large dc link capacitor due to its size, weight, volume and premature failure [10], [12]. Also, these are sensitive to electromagnetic interference (EMI) and other noises signals that may lead to short-circuit fault.

Therefore, it is required to remove the dc link capacitor, which then becomes the main attraction for MC that has very high merit over back-to-back converter like free from commutation problems, improved voltage gain with simplified control, and extremely fast transient response [10]. Also, it provides the flexibility of more control levers for independent control on frequency, voltage magnitude, phase angle and input power factor. As in wind generation system, power flow from power sources to grid, therefore traditional matrix converter with bi-directional power flow flexibility is not very much useful. Rather, indirect matrix converter (MC) after some topological modifications with lesser unidirectional switches in reversed power flow mode is of great interest for applications like WECS. Also, no additional passive components or step up transformer will be required to achieve voltage boost function.

As a generator, permanent magnet synchronous generator (PMSG) have been considered as better choice in comparison to doubly fed induction generator (DFIG) for variable speed turbine because DFIG requires gearbox, which generally suffers from faults, making the system

unreliable and costly. Moreover, PMSG has additive other merits like it has high power factor due to self excitation capability, more efficiency, light in weight, high power density, more reliable as no gearbox, more precision with simple controls, except initial installation costs [13-14]. But due to the progress made in the field of permanent magnet materials fabrication, it has extended the PMSG lifetime and decreased the production cost.

Based on above merits of unidirectional indirect reverse connected matrix converter and PMSG, this work presents experimental investigation of the developed laboratory 1.2 kW prototype of MC based wind energy conversion system. An adaptive fuzzy logic control together with space vector pulse width modulation (SVPWM) switching have been used to enhance dynamic performance under various abnormal conditions. Novelty of this work is that reversed indirect matrix converter in voltage-boosted capability with lesser no. of switches as compare to traditional matrix converter is experimentally investigated and validated for interfacing PMSG generator with grid or load. To the author's best knowledge, such configuration for WECS applications have neither addressed nor investigated before.

2. Proposed Matrix Converter Interfced Wecs

The overall block diagram of developed unidirectional indirect matrix converter (MC) and PMSG based wind energy conversion system is shown in Fig. 1.

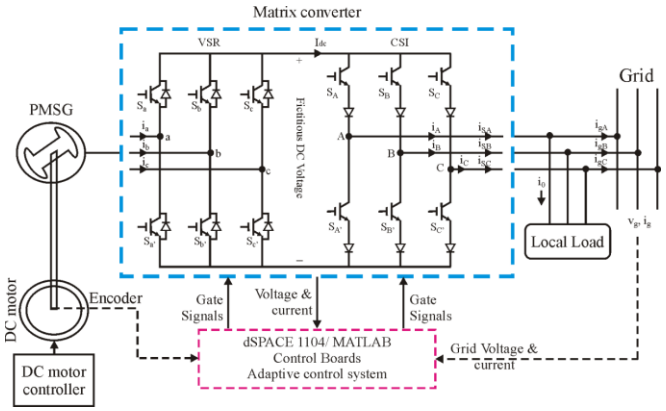

Fig. 1. Overall block diagram of the developed laboratory prototype

Here, MC interfaces PMSG with utility grid, and SVPWM switching is used to enhance dynamic performance with low harmonic and more energy yield. In this, shaft speed is controlled to achieve maximum power point tracking (MPPT) at different speeds. It also controls the pf at utility grid and fulfils the reactive power demand. In following sub-sections, different components of proposed WECS are explained.

2.1. Model of Wind Turbine

Here, in this work a wind emulator consisting of dc drive, as shown in Fig. 2 is used to drive the PMSG to perform laboratory tests under different wind and load conditions. Its control is implemented using dSPACE DS1104 real time board. It obtains the wind speed values and, then together with dc motor speed and turbine characteristics, it calculates the torque command for turbine to reproduce steady state and dynamic behavior like any practical wind turbine to conversion system.

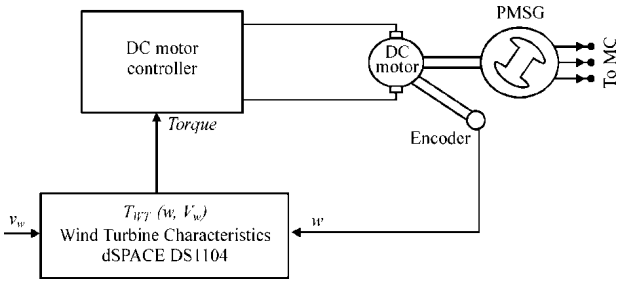

Fig. 2. Wind emulator system

The power captured ($P_{0)}$ and aerodynamic torque (T_m) by the wind turbine is expressed as [15]:

$$P_0 = 0.5\rho C_p A_r V_w^3 \quad (1)$$

$$T_m = 0.5\pi\rho C_p(\lambda) R_\omega^3 V_w^2 \quad (2)$$

where ρ is the air density, C_p is power coefficient, A_r is turbine rotor area, R_r is rotor blade radius, and V_w is wind speed.

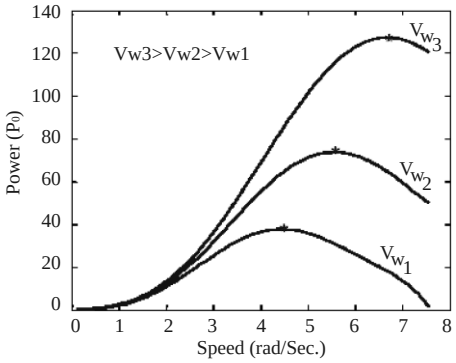

Fig. 3. Power-speed characteristics of a wind turbine at different speeds

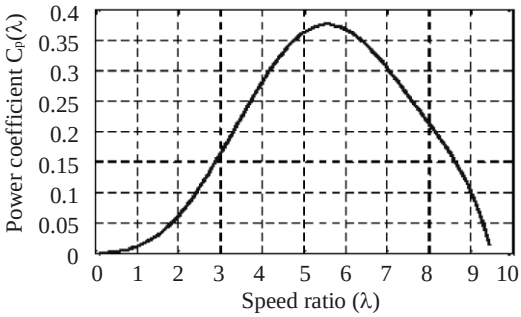

Fig. 4. C_P-λ characteristics of wind turbine

The power-speed and power coefficient - tip speed ratio characteristics of the wind turbine is illustrated in Fig. 3 and 4, respectively. The power coefficient is related to the tip speed ratio λ and rotor blade pitch angle θ according to equation (3) [15]:

$$C_p(\lambda,\theta) = 0.73\left(\frac{151}{\lambda_i} - 0.58\theta - 0.002\theta^{2.14} - 13.2\right)e^{-18.4/\lambda_i} \quad (3)$$

where

$$\lambda_i = \frac{1}{\frac{1}{\lambda - 0.02\theta} - \frac{0.003}{\theta^3 + 1}} \tag{4}$$

and

$$\lambda = \frac{\omega_m R_r}{V_\omega} \tag{5}$$

In equation (5) ω_m is the angular speed of shaft. By substituting V_W from equation (5) into (1), we get

$$P_0 = 0.5\rho C_P A_r \left(\frac{\omega_m R_r}{\lambda}\right)^3 \tag{6}$$

At any wind speed, by adjusting the shaft speed corresponding to the peak power, maximum power can be captured from wind. The novel idea explored here is to change the angular frequency through SVPWM of voltage-boosted matrix converter to track the shaft speed corresponding to maximum power point for all speeds.

2.2. Dynamic Model of Reversed Voltage-Boosted MC

Fig. 5 presents the diagram of unidirectional voltage-boosted indirect MC with twelve switches (clamping circuit is not shown here). As shown, it consists of voltage source rectifier (VSR) with anti-parallel diodes connected six switches and rare end current source inverter (CSI) with other six switches. In this topology, power flows from VSR to CSI, unlike traditional MC. This reversal in power flow is important with aspect to wind generation system as these require voltage boosting of their source power.

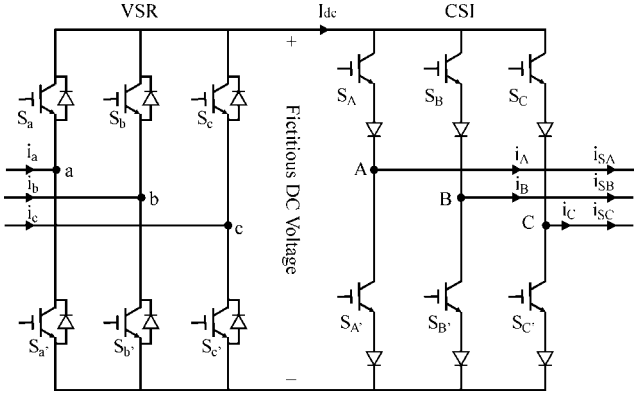

Fig. 5. Schematic diagram of the voltage boosted MC topology

The detailed modulation algorithm has been explained in detail by [10], [12], and [16-18]. At any instant, two switches (SWs) each from upper and lower group of conducts. An active state is formed when two conducting SWs are from different legs, whereas idle state is resulted when conducting SWs are from same legs. During active state, power is supplied to load, whereas during idle state circulating current flow within the MC due to shorting of fictitious dc voltage to zero. Space vector representation of CSI and VSR are shown in fig. 6, showing total three idle and six active states.

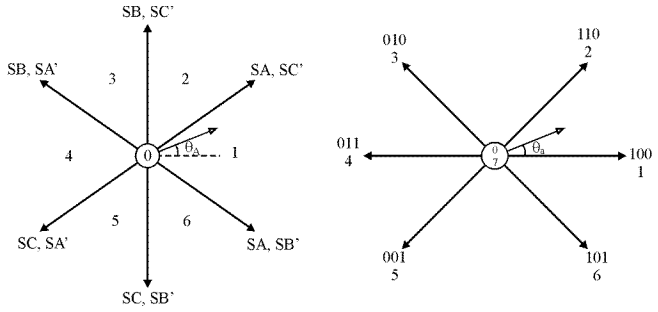

(a) CSI of MC (b) VSR OF MC

Fig. 6. Space vector representation for CSI and VSR of MC

Based on the constraints that input terminals a, b, c and output terminals A, B, C must not be short circuited and open circuited, respectively by the MC switches, the switching function for each SW can be written as:

$$S_{Kj} = \begin{cases} 1, \ switch\ S_{Kj} & closed \\ 0, \ switch\ S_{Kj} & open \end{cases} \tag{7}$$

where K = {A, B, C}, j = {a, b, c}, and

$$S_{Ka} + S_{Kb} + S_{Kc} = 1 \tag{8}$$

The relationship between instantaneous input and output phase voltages are:

$$\begin{bmatrix} v_A \\ v_B \\ v_C \end{bmatrix} = \begin{bmatrix} S_{Aa} & S_{Ab} & S_{Ac} \\ S_{Ba} & S_{Bb} & S_{Bc} \\ S_{Ca} & S_{Cb} & S_{Cc} \end{bmatrix} \begin{bmatrix} v_a \\ v_b \\ v_c \end{bmatrix} \tag{9}$$

where v_A, v_B, v_C and v_a, v_b, v_c are the output and input voltages, respectively.

From equation (9), line-to-line voltages and phase currents at terminals are:

$$\begin{bmatrix} v_{AB} \\ v_{BC} \\ v_{CA} \end{bmatrix} = \begin{bmatrix} S_{Aa} - S_{Ba} & S_{Ab} - S_{Bb} & S_{Ac} - S_{Bc} \\ S_{Ba} - S_{Ca} & S_{Bb} - S_{Cb} & S_{Bc} - S_{Cc} \\ S_{Ca} - S_{Aa} & S_{Cb} - S_{Ab} & S_{Cc} - S_{Ac} \end{bmatrix} \begin{bmatrix} v_a \\ v_b \\ v_c \end{bmatrix} \tag{10}$$

$$\begin{bmatrix} i_a \\ i_b \\ i_c \end{bmatrix} = \begin{bmatrix} S_{Aa} & S_{Ba} & S_{Ca} \\ S_{Ba} & S_{Bb} & S_{Cb} \\ S_{Ac} & S_{Bc} & S_{Cc} \end{bmatrix} \begin{bmatrix} i_A \\ i_B \\ i_C \end{bmatrix} \tag{11}$$

where v_{AB}, v_{BC}, v_{CA} and i_A, i_B, i_C are the output instantaneous voltages and currents, and i_a, i_b, i_c are instantaneous input phase currents. The averaged equivalents corresponding to (10) and (11) are:

$$\begin{bmatrix} \tilde{v}_{AB} \\ \tilde{v}_{BC} \\ \tilde{v}_{CA} \end{bmatrix} = D \begin{bmatrix} v_a \\ v_b \\ v_c \end{bmatrix} \tag{12}$$

where

$$D = \begin{bmatrix} d_{Aa} - d_{Ba} & d_{Ab} - d_{Bb} & d_{Ac} - d_{Bc} \\ d_{Ba} - d_{Ca} & d_{Bb} - d_{Cb} & d_{Bc} - d_{Cc} \\ d_{Ca} - d_{Aa} & d_{Cb} - d_{Ab} & d_{Cc} - d_{Ac} \end{bmatrix}$$

$$\begin{bmatrix} \tilde{i}_a \\ \tilde{i}_b \\ \tilde{i}_c \end{bmatrix} = \begin{bmatrix} d_{Aa} & d_{Ba} & d_{Ca} \\ d_{Ab} & d_{Bb} & d_{Cb} \\ d_{Ac} & d_{Bc} & d_{Cc} \end{bmatrix} \begin{bmatrix} i_A \\ i_B \\ i_C \end{bmatrix} \tag{13}$$

Transforming from abc to dq0 coordinates, we get:

$$f_{dq0} = T(\theta)\, f_{abc} \tag{14}$$

where $f_{dq0} = [f_d\ f_q\ f_0]^T$

$f_{abc} = [f_a\ f_b\ f_c]^T$

and

$$T(\theta) = \frac{2}{3}\begin{bmatrix} \cos\theta & \cos(\theta - \frac{2\pi}{3}) & \cos(\theta + \frac{2\pi}{3}) \\ -\sin\theta & -\sin(\theta - \frac{2\pi}{3}) & -\sin(\theta + \frac{2\pi}{3}) \\ \frac{1}{2} & \frac{1}{2} & \frac{1}{2} \end{bmatrix} \tag{15}$$

Setting, θ for input dq0 frame to $\omega_i t + \phi_i$, the input phase voltages and the corresponding dq0 quantities can be expressed as:

$$v_{dq0} = T(\omega_i t + \phi_i)\, v_{abc} \tag{16}$$

Similarly θ for output DQO frame, setting ω to $\omega_o t$, output line-to-line voltages and the corresponding DQO quantities are expressed as:

$$v_{DQO} = \frac{1}{\sqrt{3}} T\left(\omega_o t + \frac{\pi}{6}\right) v_{ABC,II} \tag{17}$$

where $v_{ABC,\,II} = [v_{AB}\ v_{BC}\ v_{CA}]^T$. Substitute for $v_{ABC,\,II}$ and v_{abc} from (16) and (17), respectively, in (12), we deduce

$$\sqrt{3}T^{-1}\left(\omega_o t + \frac{\pi}{6}\right) v_{DQO} = DT^{-1}(\omega_i t + \varphi_i) v_{dq0} \tag{18}$$

From (40), we deduce

$$v_{DQO} = \sqrt{3}T\left(\omega_o t + \frac{\pi}{6}\right) DT^{-1}(\omega_i t + \phi_i) v_{dq0} = D_{dq0}\, v_{dq0} \tag{19}$$

where D_{dq0} is defined as

$$D_{dq0} = \sqrt{3}T\left(\omega_o t + \frac{\pi}{6}\right) DT^{-1}(\omega_i t + \varphi_i) \tag{20}$$

From equations (19), and (20) we can write:

$$v_{DQ} = D_{dq}\, v_{dq} \tag{21}$$

where $v_{DQ} = [v_D\ v_Q]^T$, $v_{dq} = [v_d\ v_q]^T$

$$D_{dq} = \frac{m}{\cos\phi_i}\begin{bmatrix} \cos\phi_o\cos(\phi_i+\varphi_i) & -\cos\phi_o\sin(\phi_i+\varphi_i) \\ -\sin\phi_o\cos(\phi_i+\varphi_i) & \sin\phi_o\sin(\phi_i+\varphi_i) \end{bmatrix} \tag{22}$$

Similarly, relationship between the input and output *d* and *q*-axis quantities can be expressed as:

$$i_{dq} = D_{dq}^T\, i_{DQ} \tag{23}$$

where $i_{dq} = [i_d\ i_q]^T$, and $i_{DQ} = [i_D\ i_Q]^T$

Equations (21) and (23) present the dynamic model of the MC for WECS. The novelty of developed model is that it does not imposes restriction on the input and output frequencies. Furthermore, the model is also applicable to input/output unbalanced conditions of system.

2.3. Adaptive Fuzzy Control System

Fig. 7 presents the schematic structure of the proposed adaptive fuzzy logic control system. The control system has fuzzy controllers to control the shaft speed, incorporated with MC to yield maximum power for any wind speed by regulating the angular frequency.

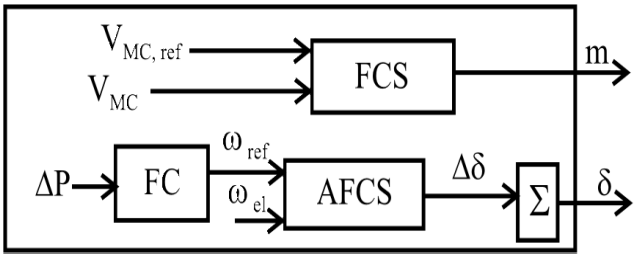

Fig. 7. Structure of angular frequency and voltage regulator

The value of ω_{ref} is dynamically achieved in real time from fuzzy controller, using P&O MPPT technique. The algorithm can be explained as below:

$$Pertubtaion: \omega_{ref}(t) = \omega_{ref}(t-1) + s\left|\Delta\omega_{ref}\right|$$

$$Observation: \Delta P_0 = P_0(t) - P_0(t-1)$$

where

$\omega_{ref}(t)$	actual angular frequency sampling
$\omega_{ref}(t-1)$	previous angular frequency sampling
$\left\|\Delta\omega_{ref}\right\|$	step of angular frequency disturb
ΔP_0	difference of power
s	search direction

This method is implemented by changing the actual angular frequency by the amount $\Delta\omega_{ref}$ and then monitoring corresponding change in output power, ΔP_0. If ΔP_0 is positive with last positive $\Delta\omega_{ref}$, the search is continued in same direction. On the other hand, if *positive* $\Delta\omega_{ref}$ causes *negative* ΔP_0, search direction is reversed. In this way, MC obtains the maximum wind power acquisition from wind turbine by driving the angular frequency ω_e, to its optimal value, ω_{ref} by regulating the active power through modulation of phase angle (δ).

The variables ΔP_0, and $\Delta\omega_{ref}$ are described by membership functions and rule table explained in [10]. Finally, this searching method drives ω_{ref} to oscillate near the optimum value for the current wind speed.

The angular frequency of generator, ω_e, is monitored, compared with current reference value, ω_{ref}, and then error is sent to the Adaptive Fuzzy Control System (AFCS), which generates the SVPWM phase angle "δ" as shown in Fig. 7. For example, when AFCS detects that value of electrical frequency, ω_e, is below the optimal value, it generates a negative value of phase angle "$\Delta\delta$" for MC, which results in the decrease of "δ", and in turn less power absorbed as

closed loop control commands the decreases of excitation current which in turn reduces the air-gap magnetic field. All the control objectives are achieved through improved SVPWM based reversed indirect matrix converter. Control algorithm has been developed in MATLAB/Simulink programming environment using dSPACE DS1104 kit.

3. Experimental Results and Discussion

Laboratory 1.2 kW prototype of reversed MC based wind energy conversion system has been built (shown in Fig. 8), using the MATLAB/Simulink and dSPACE DS1104, in order to allow real time control for experimental investigation under different conditions.

The LC filter between the MC and the grid consists of inductance of 1.5 mH and a capacitor of 12.5 µF. The laboratory prototype is investigated under different input/output conditions like abrupt change in wind speed, disconnection from grid, misfire in the converter, sudden out of one phase, change in load etc.

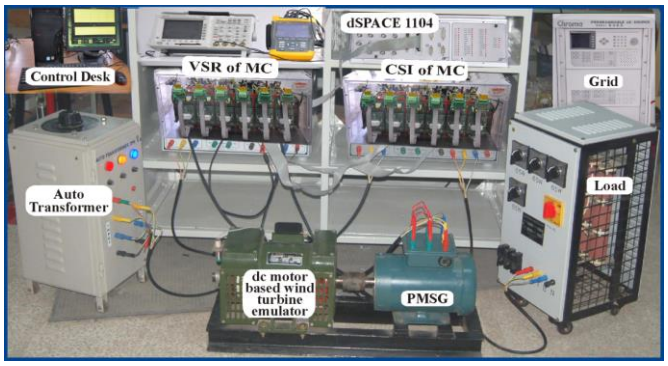

Fig. 8. Schematic of experimental setup of MC interfaced PMSG for WECS

3.1. Response under Steady-state

In grid-connected mode, the main aim of proposed control algorithm is to track the dispatch power so as to yield maximum energy. Fig. 9 shows the experimental waveforms of grid phase voltage and current for unity, lagging and leading pf operations. It demonstrates the reactive power capability of the MC for wind power applications. The reactive power can be controlled for unity, lagging and leading pf operation, while keeping active power constant as shown in Fig. 10, illustrating the reactive power control capability of the proposed system.

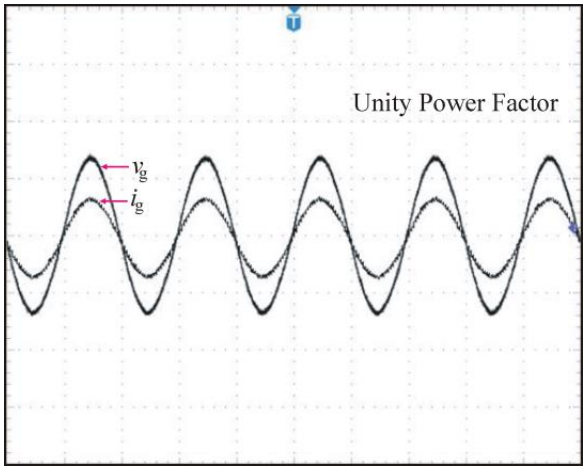

(a)

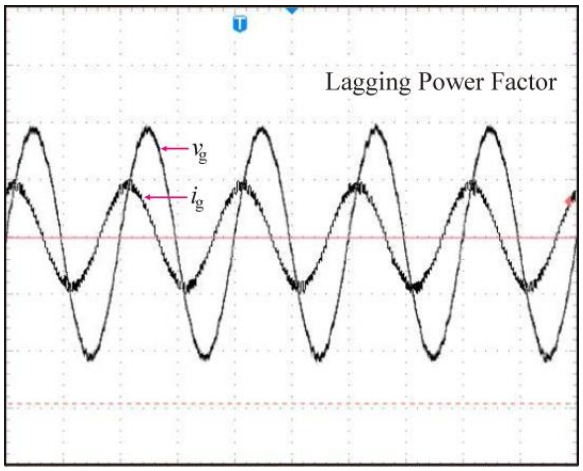

(b)

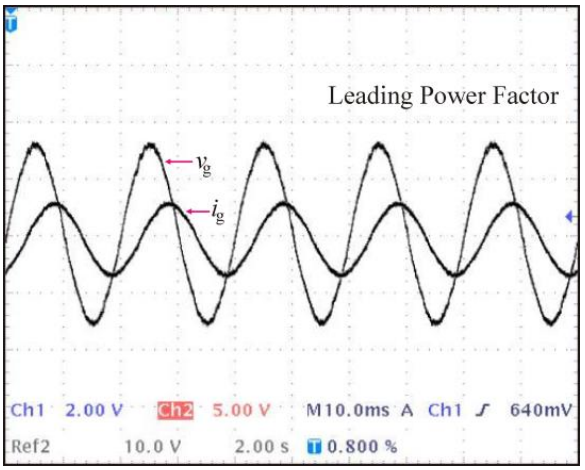

(c)

Fig. 9. Experimental waveform of grid phase voltage v_g and injected grid current i_g during steady-state for (a) Unity power factor operation, (b) Lagging power factor operation, and (c) Leading power factor operation.

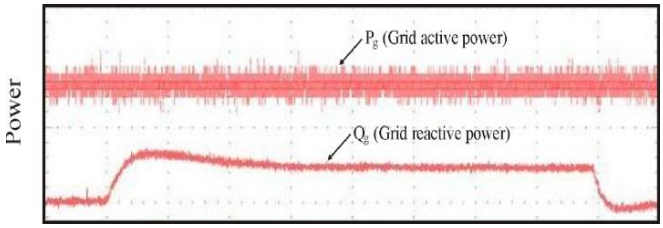

Fig. 10. Experimental waveform of grid active and reactive power.

Fig. 11 shows the experimental waveforms of fictitious dc current i_{dc}; unfiltered MC output current i_A; grid phase voltage v_g and injected grid current i_g during steady-state condition. Fig. 12 presents the harmonic spectrum for injected grid current and voltage, where it can be seen that total harmonic distortion (THD) is 2.4% and 2.3%, respectively. It can be observed from Fig. 11 and 12 that grid injected phase current and voltages are well regulated sinusoidal with almost unity power factor. Also, pf is equal to 0.996 and total harmonic distortion (THD) is 2.3%, which satisfies the pf demand, and is far better as compare to pf and THD of 0.94% and 4.25%, respectively in case of converter topology proposed for wind power applications in [19].

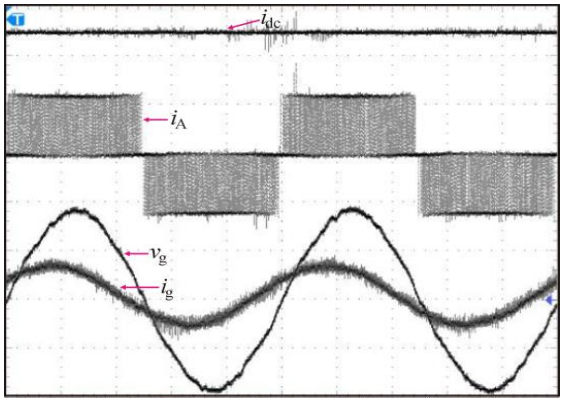

(a)

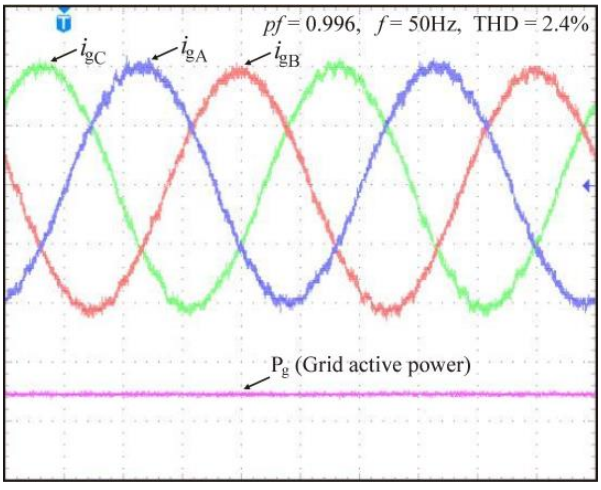

(b)

Fig. 11. Experimental waveform during steady-state condition. (a) fictitious dc current i_{dc}; unfiltered MC output current i_A; grid phase voltage v_g and injected grid current i_g and (b) three-phase grid phase voltages v_{gA}, v_{gB}, v_{gC}; grid output active power P_g .

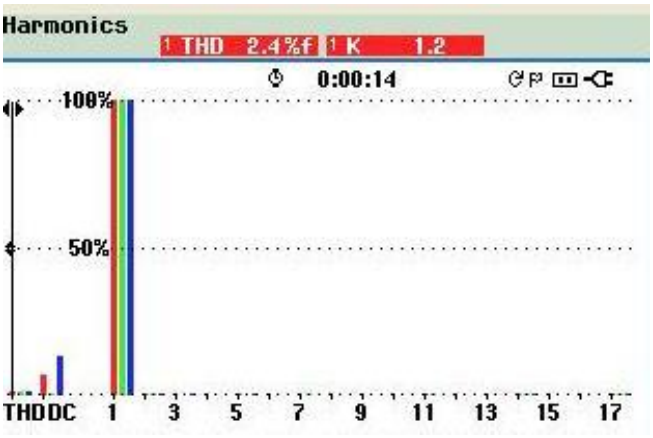

(a)

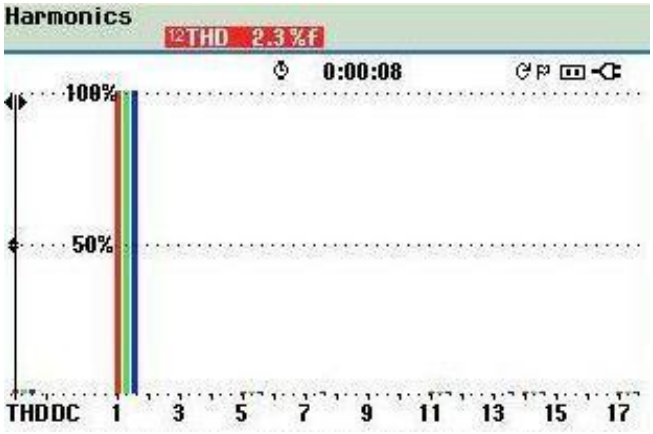

(b)

Fig. 12. Harmonic spectrum for injected grid current i_{gA} and grid voltage v_g ((a)Injected grid current $i_{gA,}$ (b) Grid voltage (v_g)

The THD measured for grid injected current and voltage is quite low as per IEEE 1547, IEEE-519 and IEC 61727 standard and thus satisfies the general standards of produced power in terms of voltage and current THDs within the limits of 5%. Such improvement in pf results into reduction of around 13% generator conduction losses. It demonstrates expected improvement when compared with similar works. It is clear that this proposed optimal controller for matrix converter interfaced WECS succeeds in regulating the load voltage and frequency within satisfied limits of 220/400V and 50Hz respectively.

3.2. Response under Dynamic Conditions

Fig. 13 and 14 validates the effectiveness of proposed controls for developed laboratory prototype of WECS during various dynamic conditions. Fig. 13 shows the response of load voltage, rms line current, MC output current, load current, fictitious dc link voltage under varying load conditions. Here, the load is changed from 100% to 50% and back to 100% to simulate the transient load changing. It can be seen that load voltage is well-maintained despite variations in load. But, load current changes with load as expected. Therefore, verifying that the proposed controller regulates the load voltage and frequency effectively under varying load conditions.

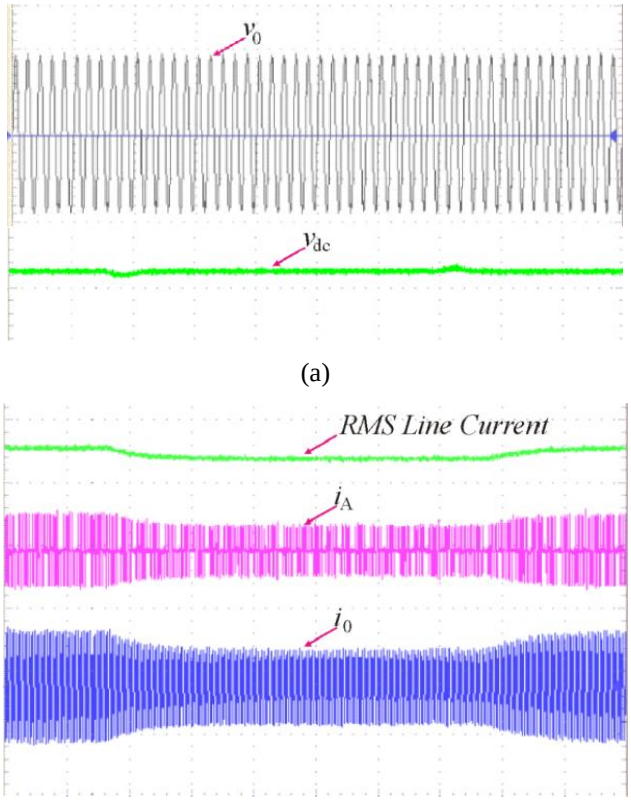

Fig.13. Experimental waveform during varying load condition: (a) load voltage, and fictitious dc link voltage (b) RMS line current, MC output current, and load current response when the load changes from 100% to 50% and then from 50% to 100%.

It can be noticed that when load is decreased, load current also decreases, and so closed loop control commands the necessary control action to maintain the constant voltage magnitude. Whereas, when load is increased, load current also increases, but the controller keeps the load voltage constant, as expected. The experimental waveforms illustrates that developed WECs is able to stabilize load voltage under varying load conditions by regulating modulation index of MC.

The proposed control algorithm for MC interfaced WECS is also tested experimentally when current commands is increased and decreased. Fig.14 illustrates the dynamic responses of injected grid currents to the grid when input current commands of MC are decreased from 3.5A to 1.5A, and increased from 1.5A to 3.5A respectively.

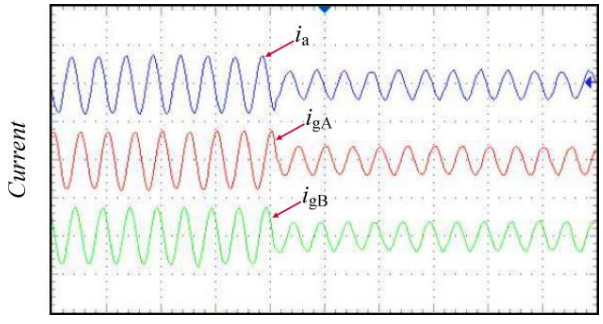

(a) Current command decreasing

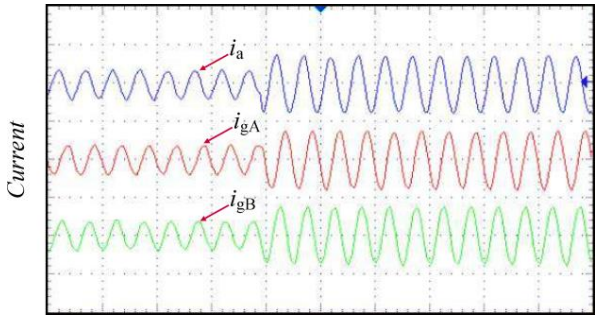

(b) Current command increasing

Fig. 14. Experimental waveforms of PMSG output voltage, input grid phase voltage, MC input phase currents and injected grid current sowing dynamic response during (a) decrease of MC current command; and (b) increase of MC current command.

From the experimental waveforms, it can be noticed that unity pf is maintained, despite of dynamic current command changing. Also, input current of MC can track effectively its current commands. The injected grid current decreases or increases accordingly without deteriorating the waveforms.

4. Conclusion

This paper presents the effectiveness of the use of reversed voltage boosted MC for WECS in terms of low harmonic characteristics and enhanced dynamic performance through laboratory prototype setup and validates its robustness experimentally under various dynamic and steady-state conditions. The SVPWM based reversed voltage boosted MC is able to maintain the magnitude and frequency of grid/or load voltage and current under different load conditions. Results show that output current and voltage of MC injected to the grid or load satisfies IEC 61727 and IEEE 519 standards demonstrating excellent steady-state and dynamic performance of the proposed controls.

Appendix

DC shunt motor
Armature voltage= 180 V; Armature current=8A
Field voltage=220V; Field current=0.5A
Rated speed=1500rpm; Rated Power=1.5HP
PMSG generator
Voltage= 230/460 V; Current=2.6/1.2A; No. of poles=4
Rated speed=1800rpm; frequency=50 Hz

References

[1] R. C. Portillo , M. M. Prats and J. I. Leon "Modelling strategy for back-to-back three-level converters applied to high-power wind turbines", *IEEE Transaction Ind. Electron.*, vol. 53, no. 5, pp.1483 -1491 2006

[2] R. Pena, J.C. Clare, and G.M. Asher, "A doubly fed induction generator using back-to- back PWM converters supplying an isolated load from a variable speed wind turbine", *IEE Proc.- Electric Power Applications*, vol. 143, no. 5, Sep. 1996 pp.:380 – 387.

[3] P. Rodriguez, A.V.Timbus, R.Teodorescu, M.Liserre and F. Blaabjerg "Flexible active power control of distributed power generation systems during grid faults", *IEEE Transaction Ind. Electron.*, vol. 54, no. 5, pp. 2583 - 2592, 2007.

[4] R. Teodorescu and F. Blaabjerg, "Flexible control of small wind turbines with grid failure detection operating in stand-alone and grid- connected mode", *IEEE Transaction Power Electronics*, vol. 19, no. 5, Sep. 2004, pp. 1323, 1332.

[5] S. Muller , M. Deicke and R. W. De Doncker "Doubly fed induction generator systems for wind turbine", *IEEE Ind. Appl. Mag.*, vol. 8, no. 3, pp.26 -33 2002

[6] A. Garcés, M. Molinas, "A Study of Efficiency in a Reduced Matrix Converter for Offshore Wind Farms", *IEEE Transactions on Industrial Electronics*, vol. 59, no. 1, pp. 184 – 193, Jan. 2012.

[7] R. Cardenas, R. Pena, P. Wheeler, J. Clare, and G. Asher, "Control of the reactive power supplied by a WECS based on an induction generator fed by a matrix converter," IEEE *Transaction* Ind. Electron., vol. 56, no. 2, pp. 429–438,Feb. 2009.

[8] H. Nikkhajoei and M. Iravani, "A matrix converter based micro-turbine distributed generation system," IEEE *Transaction* Power Del., vol. 20, no. 3, pp. 2182–2192,Jul. 2005.

[9] R. Cárdenas, R. Pen¸a, J. Clare, and P. Wheeler, "Analytical and experimental evaluation of a WECS based on a cage induction generator fed by a matrix converter," IEEE *Transaction* Energy Convers., vol. 26, no. 1, pp. 204–215, Mar. 2011.

[10] V. Kumar, R. R. Joshi, and R. C. Bansal, "Optimal control of matrix-converter-based WECS for performance enhancement and efficiency optimization," IEEE *Transaction* Energy Conversion, vol. 24, no. 1, pp. 264–273, Mar. 2009.

[11] S. M. Barakati, M. Kazerani, and J. D. Aplevich, "Maximum power tracking control for a wind turbine system including a matrix converter," IEEE *Transaction* Energy Conversion,vol.24,no.3,pp.705–713,Sep. 2009.

[12] Fang Gao, and M. Reza Iravani, "Dynamic model of a space vector modulated matrix converter", *IEEE Transaction Power Delivery*, vol. 22, no. 3, Jul..2007, pp. 1696-1705.

[13] M. Chinchilla, S. Arnaltes, and Burgos, "Control of permanent-magnet generators applied to variable-speed wind-energy systems connected to the grid", IEEE *Transaction* of Energy Conversion, vol. 21, no.1, Mar. 2006, pp. 130-135.

[14] K. H. Kim, Y. C. Jeung, D. C. Lee, and H. G. Kim, "LVRT scheme of PMSG wind power systems based on feed- back linearization," IEEE *Transaction* Power Electron., vol. 27,no.5, pp.2376–2384,May 2012.

[15] J. G. Slootweg, S. W. H. de Haan, H. Polinder, and W. L. Kling, "General model for representing variable speed wind turbines in power system dynamics simulations", *IEEE Transaction Power Systems*, vol. 18, no. 1, Feb.2003, pp. 144-151.

[16] J. Chang, T. Sun, and A. Wang, "Highly compact AC-AC converter achieving a high voltage transfer ratio," *IEEE Transaction Ind. Electron.*, vol. 49, pp. 345–352, Apr. 2002.

[17] P. W. Wheeler, *IEEE*, J. Rodríguez, J. Clare, L. Empringham, and A. Weinstein, "Matrix converters: a technology review", *IEEE Transaction Power Electronics*, vol. 49, no. 2, Apr. 2002, pp. 276-289.

[18] X.Liu, P. C. Loh, P. Wang, F.Blaabjerg, Y. Tang, and E. A. Al-Ammar, "Distributed generation using indirect matrix converter in reverse power mode", IEEE *Transaction* on Power Electron., vol.28,no.3,pp.1072–1082, Mar. 2013.

[19] D.S. Oliveira, M.M.Reis, C.E.A. Silva, L.H.S. Colado Barreto, F. L.M. Antunes, and B. L. Soares, "A three-phase high frequency semi-controlled rectifier for PM WECS", IEEE *Transaction* on Power Electronics, vol.25,no.3,pp.677–685, Mar. 2010.